

Impaired ATP Synthase Assembly Associated with a Mutation in the Human ATP Synthase Subunit 6 Gene*

Received for publication, September 5, 2000, and in revised form, October 26, 2000
Published, JBC Papers in Press, November 13, 2000, DOI 10.1074/jbc.M008114200

Leo G. J. Nijtmans^{‡§¶}, Nadine S. Henderson^{‡¶||}, Giuseppe Attardi^{**}, and Ian J. Holt^{||‡‡}

From the [‡]Department of Molecular Pathology, University of Dundee, Ninewells Medical School, Dundee DD1 9SY, United Kingdom, ^{||}Dunn Human Nutrition Unit, Wellcome Trust, Cambridge CB2 2XY, United Kingdom, and the ^{**}Division of Biology, California Institute of Technology, Pasadena, Los Angeles, California 91125.

Mutations in human mitochondrial DNA are a well recognized cause of disease. A mutation at nucleotide position 8993 of human mitochondrial DNA, located within the gene for ATP synthase subunit 6, is associated with the neurological muscle weakness, ataxia, and retinitis pigmentosa (NARP) syndrome. To enable analysis of this mutation in control nuclear backgrounds, two different cell lines were transformed with mitochondria carrying NARP mutant mitochondrial DNA. Transformant cell lines had decreased ATP synthesis capacity, and many also had abnormally high levels of two ATP synthase sub-complexes, one of which was F₁-ATPase. A combination of metabolic labeling and immunoblotting experiments indicated that assembly of ATP synthase was slowed and that the assembled holoenzyme was unstable in cells carrying NARP mutant mitochondrial DNA compared with control cells. These findings indicate that altered assembly and stability of ATP synthase are underlying molecular defects associated with the NARP mutation in subunit 6 of ATP synthase, yet intrinsic enzyme activity is also compromised.

ATP synthase (or complex V) is the enzyme of aerobic ATP production. It is located in the inner mitochondrial membrane of eukaryotic cells together with four respiratory chain enzymes that generate the proton motive force, which in turn drives ATP synthesis. ATP synthase comprises a rotary catalytic portion, F₁-ATPase, whose structure has been solved (1), a transmembrane portion F₀, and two stalks that link F₁ and F₀. Two of the subunits of the F₀ portion of ATP synthase, subunits 6 and 8 (or subunit a and A6L), are encoded in mitochondrial DNA in all animal cells. Specific inhibition of mitochondrial translation (including subunits 6 and 8) by drug treatment leads to accumulation of two ATP synthase assembly intermediates and a concomitant decrease in holoenzyme in human cultured cells (2).

* This work was supported by the European Union in the form of a Training and Mobility of Researchers fellowship (to L. N.), the Scottish Hospital Endowments Research Trust, and the Medical Research Council. The costs of publication of this article were defrayed in part by the payment of page charges. This article must therefore be hereby marked "advertisement" in accordance with 18 U.S.C. Section 1734 solely to indicate this fact.

§ Current address: Section for Molecular Biology, Dept. of Molecular Biology, University of Amsterdam, Kruislan 318, 1098 SM Amsterdam, the Netherlands.

¶ Contributed equally to this work.

‡‡ A Royal Society University Research Fellow (1992–1999). This study was initiated when I. Holt was a Lucille Markey Visiting Fellow in the laboratory of G. Attardi. To whom correspondence should be addressed: Dunn Human Nutrition Unit, Wellcome Trust-MRC Bldg., Hills Rd. Cambridge, CB2 2XY, UK. Tel.: 44 12 23 25 28 40; Fax: 44 12 23 25 28 45; E-mail: ih@mrc-dunn.cam.ac.uk.

One of the earliest disease-associated point mutations of mtDNA¹ to be described was localized to ATP synthase subunit 6 gene, hereafter called A6 (3). The mutation, a thymine to guanine transversion at nucleotide position 8993 of human mtDNA, hereafter termed T8993G, predicts substitution of a highly conserved leucine by arginine at amino acid position 156. The mutation was found in a family presenting with neurogenic muscle weakness, ataxia, and retinitis pigmentosa, a syndrome termed NARP. There was good correlation between mutant load and disease severity (3). This was further documented when it was shown that very high levels of T8993G mutant mtDNA were associated with a severe neurodegenerative disease of childhood (maternally inherited Leigh syndrome, or MILS) (4). The T8993G mtDNA mutation is found in ~15% of patients with a mitochondrial disorder whose disease has been clearly linked to a point mutation in mtDNA.² Considered collectively, mitochondrial disorders are among the commonest neurological diseases; therefore the mutation is of considerable clinical importance.

In the current structural model of mitochondrial ATP synthase, the enzyme represents a rotary motor (1). A6 forms part of one of the stators, and subunit c forms the rotor (5). The T8993G mtDNA mutation predicts an arginine for leucine substitution in the fourth helix of A6, a region that is believed to interact with subunit c. A second point mutation at nucleotide position 8993 changes leucine to proline and is associated with a similar phenotype in patients (6). Thus, it is likely that any amino acid substitution in this region that induces a conformational change will perturb holoenzyme activity, assembly, or stability.

The T8993G mtDNA mutation did not appear to alter ATP hydrolysis activity (4) but did decrease ATP synthesis in digitonin-permeabilized cells (7). Subsequently, Wallace and co-workers (8) use 143B osteosarcoma cells that lack mtDNA (ρ^0 cells) as recipients of mitochondria carrying T8993G mtDNA. They found that mitochondria with T8993G mtDNA, isolated from this control nuclear background, had reduced state III respiration, indicative of decreased ATP synthase activity. In another study, muscle mitochondria harboring T8993G mtDNA were shown to contain sub-complexes of ATP synthase, raising the possibility that the underlying defect in this disease was holoenzyme assembly or stability (9). Here we demonstrate for the first time that mutant subunit A6 of ATP synthase is linked to impaired assembly of complex V in human cells.

¹ The abbreviations used are: mtDNA, mitochondrial DNA; NARP, neurological muscle weakness, ataxia, and retinitis pigmentosa; BN-PAGE, blue native-polyacrylamide gel electrophoresis; Bis-Tris, 2-[bis(2-hydroxyethyl)amino]-2-(hydroxymethyl)propane-1,3-diol; DMEM, Dulbecco's modified Eagle's medium; MOPS, 4-morpholinopropanesulfonic acid; OP, oxidative phosphorylation.

² M. Zeviani, personal communication.

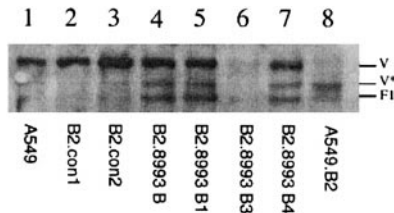


FIG. 1. Mitochondrial membrane fractions prepared from NARP cybrids contained increased levels of ATP synthase sub-complexes. Proteins from crude mitochondrial preparations were separated by BN-PAGE on a 5–12% polyacrylamide gradient gel. Protein was transferred to solid support and immunoblotted with human F_1 -ATPase antibodies. V, ATP synthase holoenzyme, F_1 , F_1 -ATPase; V^* , a sub-complex of complex V that includes F_1 -ATPase and subunit c. Lane 1, A549 lung carcinoma cells; lanes 2 and 3, control lung carcinoma cybrids; lane 4, lung carcinoma cybrid clone B2.8993 B; lanes 5–7, sub-clones of cybrid B2.8993B; lane 8, lung carcinoma (A549.B2) ρ^0 cells. Control cybrids were generated by fusing cytoplasts derived from fibroblasts of a normal control subject with lung carcinoma ρ^0 cells. B2.8993 denotes the transformant cybrid lines produced by fusing lung carcinoma ρ^0 cells (A549.B2) with cytoplasts derived from NARP fetal fibroblasts.

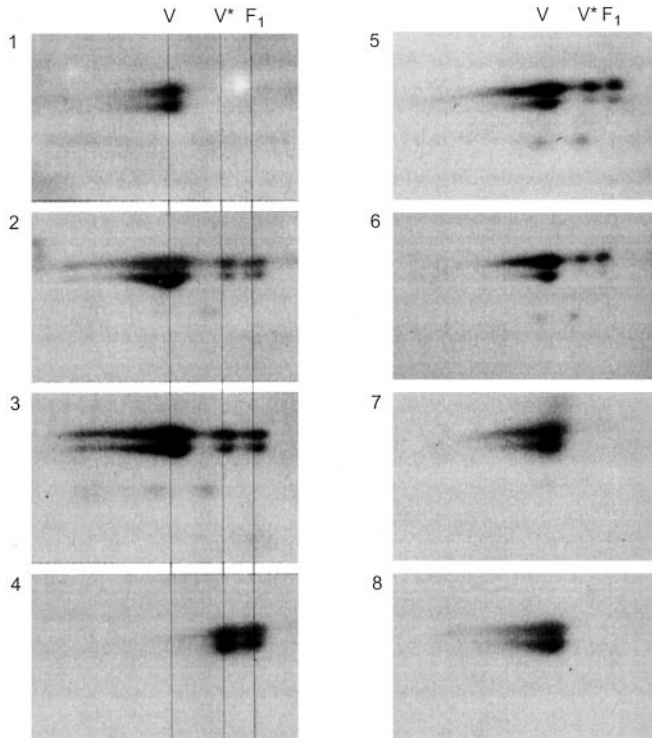


FIG. 2. ATP synthase appeared structurally normal in some lung carcinoma NARP cybrids, whereas complex V sub-complexes were always present in osteosarcoma NARP cybrids. Each panel is a mitochondrial membrane sample separated in the first dimension by BN-PAGE (left to right) and subsequently in a second dimension 12% denaturing SDS-PAGE (top to bottom). Protein was transferred to solid support and immunoblotted with the same F_1 -ATPase antibodies used in Fig. 1. Panel 1, 143B osteosarcoma mitochondrial; panels 2 and 3, typical osteosarcoma NARP cybrids (two of five screened) showing increased amounts of F_1 -ATPase and V^* . Panel 4, mitochondria derived from 206 ρ^0 osteosarcoma cells. Panels 5–8, four lung carcinoma NARP cybrids, two of which appeared structurally normal (panels 7 and 8), whereas two displayed abnormally high levels of F_1 -ATPase and V^* (panels 5 and 6).

MATERIALS AND METHODS

The standard cell culture medium in this study was Dulbecco's modified Eagle's medium (DMEM) containing 4.5 g/liter glucose, 110 mg/liter pyruvate, with 10% fetal bovine serum. Tissue culture reagents were purchased from Life Technologies, Inc. The osteosarcoma 143B TK⁻ cells and cybrids were supplemented with 100 μ g/ml bromodeoxyuridine. The ρ^0 cells derived from the osteosarcoma 143B cell line

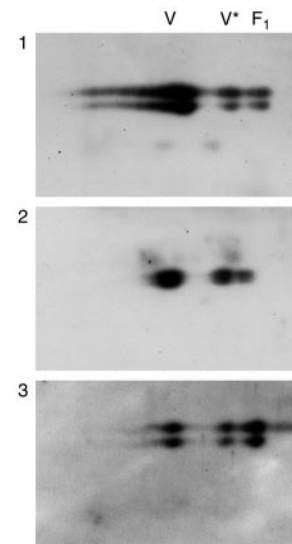


FIG. 3. The amount of ATP synthase sub-complexes was variable for a particular clone. There was some experiment-to-experiment variation in the level of complex V sub-complexes. This was seen most dramatically with osteosarcoma cybrid clone 206.8993A. Mitochondrial membrane fractions were prepared and separated by the standard protocol in all cases. Panel 1 is reproduced from Fig. 2, panel 3; panels 2 and 3 are separate mitochondrial preparations from the same clonal cell line. The relative amount of sub-complexes was appreciably higher in panel 2 than panel 1, and in the case of the sample shown in panel 3, F_1 -ATPase was the major form detected. The variation is attributed to holoenzyme disassembly occurring during isolation and sample preparation. The relative signals from ATP synthase holoenzyme (V), V^* , and F_1 -ATPase were, respectively, 75:12:13 (panel 1), 60:24:16 (panel 2), and 37:16:47 (panel 3).

(143B.206) and the lung carcinoma cell line (A549.B2) were in addition supplemented with 50 μ g/ml uridine. The absence of mtDNA from both these cell lines has been shown previously by Southern blotting and polymerase chain reaction (10, 11).

Enucleation of cells was achieved by inverting 35-mm tissue culture plates, 70–90% confluent, in 95% DMEM, 5% fetal bovine serum with 10 μ g/ml cytochalasin B (Calbiochem) and centrifuging at $7,000 \times g$ for 20 min. The resultant cytoplast lawn was incubated for 3 h at 37 $^{\circ}$ C with $\sim 8 \times 10^5$ ρ^0 cells. The addition of 50% w/v polyethylene glycol 1500, 45% DMEM, 5% Me₂SO induced cell-cytoplast fusion. After 1 min, the cells were washed twice in 90% DMEM, 10% Me₂SO and three times in DMEM alone and incubated overnight in 90% DMEM, 10% fetal bovine serum without uridine. Putative transformant cells were re-plated on 90-mm dishes in 90% DMEM, 10% fetal bovine serum without uridine. Individual colonies were picked ~ 14 days later using glass rings. Cytoplast- ρ^0 cell fusion was performed between NARP fetal fibroblasts after enucleation and osteosarcoma or lung carcinoma ρ^0 cells. Transformant osteosarcoma cybrids carrying mtDNA molecules derived from NARP fetal fibroblasts were designated 206.8993. Equivalent lung carcinoma cybrids were denoted B2.8993. In addition, cybrids carrying mtDNA from a control subject were generated by the same protocol and designated 206.con (osteosarcoma cybrids) or B2.con (lung carcinoma cybrids).

Blue native electrophoresis (BN-PAGE) and second dimension SDS-PAGE were performed using the method of Schagger and Von Jagow (13) and Schagger *et al.* (14). Mitochondrial samples were prepared by incubating 5×10^6 cells in 200 μ l of phosphate-buffered saline with 2 mg/ml digitonin for 10 min on ice. The solution was centrifuged at $12,000 \times g$ for 4 min at 4 $^{\circ}$ C, and the resultant crude mitochondrial pellet was washed once with phosphate-buffered saline, re-centrifuged, and stored at -70 $^{\circ}$ C. Immediately before electrophoresis, the mitochondrial pellet was resuspended in 100 μ l of 1.5 M 6-aminohexanoic acid, 50 mM Bis-Tris, pH 7.0, with 20 μ l of 10% *n*-dodecyl maltoside and incubated on ice for 15 min. After centrifugation at $12,000 \times g$ for 20 min at 4 $^{\circ}$ C, the supernatant was mixed with 10 μ l of 5% Serva Blue G in 1 M 6-aminohexanoic acid, and equal amounts of protein, as determined by the Bradford method (15), were added to each lane of a 5–13% gradient gel.

Pulse-chase experiments were performed as described previously. (16). Exponentially growing cells in DMEM without methionine (ICN)

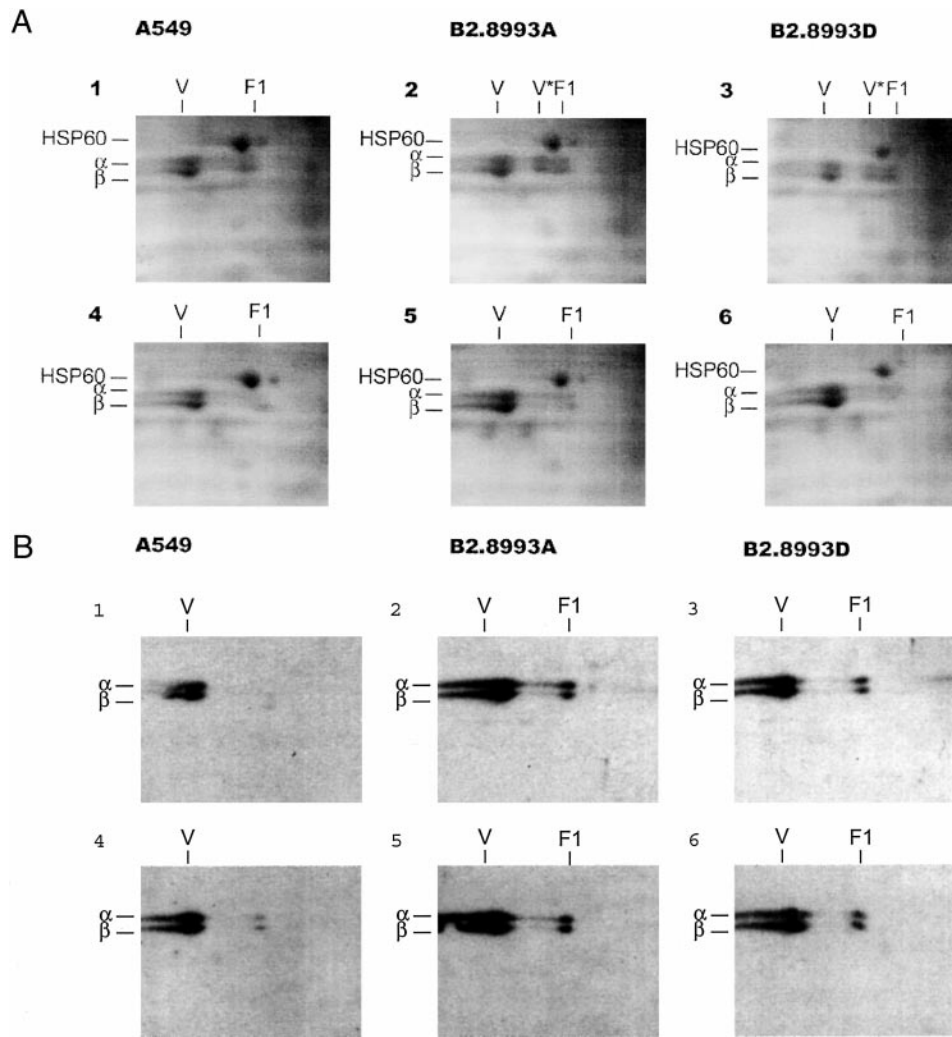


FIG. 4. Comparison of the levels of newly synthesized and steady-state complex V holoenzyme and sub-complexes indicated a decreased rate of enzyme assembly in lung carcinoma NARP cybrids compared with controls. ^{35}S -Labeled protein after a 1-h pulse and a chase of 1 h (panels 1, 2, and 3) or 3 h (panels 4, 5, and 6) was separated in the first dimension by BN-PAGE and in the second dimension by SDS-PAGE. The area of the gels shown includes α and β subunits of ATP synthase and its sub-complexes for a control (panels 1 and 4) and lung carcinoma NARP cybrids B2.8993 A (panels 2 and 5) and D (panels 3 and 6). *B*, immunoblots of the samples shown in *A*. The antibody was to F_1 -ATPase, *i.e.* the same as that used in Figs. 1–3 above. In the examples shown, two identical gels were prepared for each time point; one was immunoblotted, and the second was dried and exposed to x-ray film. In other experiments, radiolabeled protein was transferred to solid support, and immunoblotting and x-ray film detection were then performed from a single gel. The results were similar; however, with the latter approach, there was a slight decrease in signal from ^{35}S -labeled protein. Note that radiolabeled V^* was detected in NARP cybrids after a 1-h chase, yet this sub-complex did not appear on the equivalent immunoblot. Thus, the inference is that the transition from V^* to fully assembled complex V, which involves incorporation of A6, is delayed in NARP cybrids. HSP60 is a useful marker as it bisects V^* and F_1 -ATPase on first dimension BN-PAGE and runs slightly behind the α and β subunits of F_1 -ATPase on second dimension SDS-PAGE.

were incubated with [^{35}S]methionine at a final concentration of 20 $\mu\text{Ci}/\text{ml}$. After chase times of 0, 1, 3, 6, and 18, h cells were harvested and used to prepare crude mitochondrial fractions (17) for two-dimensional BN-PAGE. The gels were fixed, treated with AmplifyTM (Amersham Pharmacia Biotech) according to the protocol of the manufacturer, dried, and exposed to x-ray film for 1–24 h at -70°C . Alternatively, in some instances labeled protein was transferred to Hybond-C membrane and exposed to x-ray film, as for the dried gels, after which the membrane was blocked and immunoblotted with antibody to subunits of F_1 -ATPase. A Molecular Dynamics Personal Densitometer SI was used to quantify the relative amounts of each complex.

The rate of ATP synthesis in cybrids was determined using the method of (18). Briefly, cells were harvested and resuspended at 1×10^6 cells/ml in incubation buffer including 20 $\mu\text{g}/\text{ml}$ digitonin. Permeabilized cells were incubated with succinate (5 mM) and rotenone (4 $\mu\text{g}/\text{ml}$) for 15 min at 37°C . Reactions were stopped by the addition of perchloric acid. After incubation on ice for 2 min, samples were centrifuged at $13,000 \times g$ for 2 min, and the supernatants were neutralized with 2 M KOH, 0.6 M MOPS. The samples were re-centrifuged, and 1–5- μl aliquots of the final supernatant combined with 50 μl of ATP monitoring reagent (Bio-Orbit, Turku, Finland). The amount of light detected in a luminometer was converted to moles of ATP with reference to ATP

standards after deducting the signal obtained from the corresponding ρ^0 cells (osteosarcoma or lung carcinoma). Thus, the values obtained reflect ATP synthesis activity that was specific to oxidative phosphorylation (OP). Histochemical staining of ATP hydrolysis activity in blue native polyacrylamide gels was performed according to Zerbetto *et al.* (19).

Growth rates were assessed either by direct counting of trypsinized cells on a Neubauer counting chamber or using a tetrazolium salt (3-(4,5-dimethylthiazol-2-yl)-2,5-diphenyltetrazolium bromide) that acts as a vital dye. (20). Cells were grown in DMEM with 4.5 g/liter glucose or DMEM with 0.9 g/liter galactose substituted for glucose. Intact cell oxygen consumption rates were determined in a Clark-type oxygen electrode from 500–1000 μl of 5×10^6 cells/ml in RPMI 1640 medium without glucose (Life Technologies). Oxygen consumption rates were expressed as fmol of $\text{O}_2/\text{min}/\text{cell}$. The addition of carbonyl cyanide *p*-chlorophenylhydrazone or carbonyl cyanide *p*-trifluoromethoxyphenylhydrazone during an experiment led to an increase in the rate of oxygen consumption in all cells tested (data not shown), indicating that the assay was measuring coupled respiration. DNA extraction, amplification, electrophoresis, blotting, and hybridization were as described (39). For quantification of the level of mutant mtDNA, DNA was extracted from $\sim 5 \times 10^6$ cells and digested with *Ava*I, and the restriction

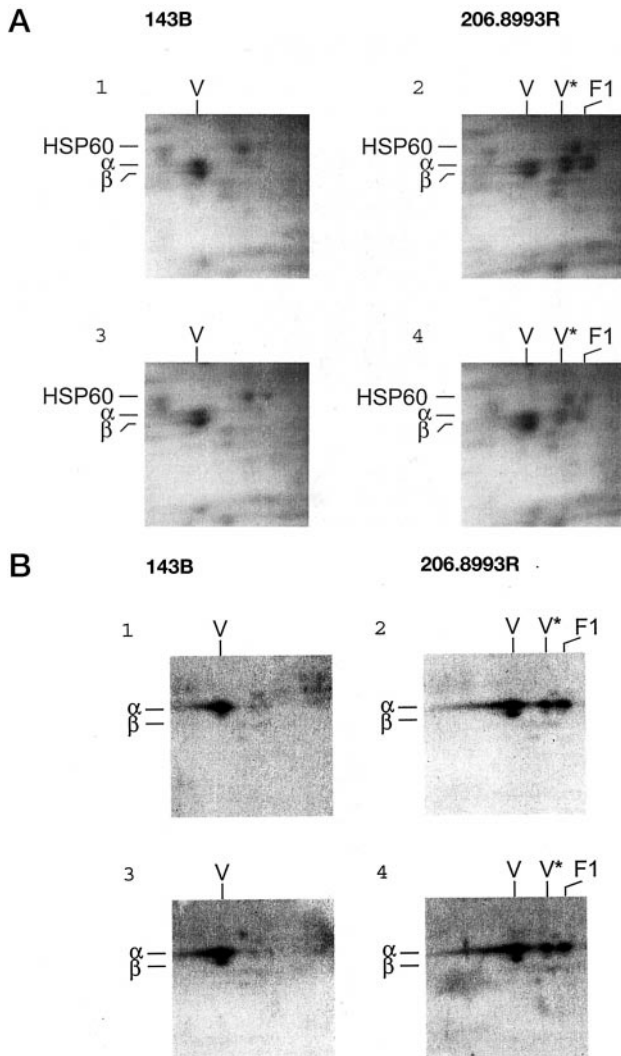


FIG. 5. Comparison of the levels of newly synthesized and steady-state complex V holoenzyme and sub-complexes in an osteosarcoma NARP cybrid indicate impaired holoenzyme assembly. A, ^{35}S -labeled protein after a 1-h pulse and a chase of 3 h (panels 1 and 2) or 18 h (panels 3 and 4) was analyzed as described in Fig. 4. The area of the gels shown includes α and β subunits of ATP synthase and its sub-complexes for a control (panels 1 and 3) and an osteosarcoma NARP cybrid (panels 2 and 4). B, immunoblots of the samples shown in A. ATP synthase holoenzyme accounted for the vast majority (95–98%) of the signal from radiolabeled α and β subunits (A) and immunoblots of α and β subunits (B) in the control cells. In the osteosarcoma NARP cybrid, the steady-state proportion of holoenzyme to sub-complexes was similar after 3 and 18 h, 74:26 and 72:28, respectively. In contrast, although after an 18-h chase, the proportions were similar (70:30) for radioisotope-labeled α and β subunits, after 3 h the ratio was 34:66, indicating that the labeled subunits were not assembled into ATP synthase holoenzyme at the rate seen in control cells.

fragments were separated on 1% agarose gels. After Southern blotting, filters were probed with total purified human mtDNA. Mitochondrial translation products were labeled specifically by incubating 10^6 cells with $250 \mu\text{Ci/ml}$ [^{35}S]methionine (PerkinElmer Life Sciences) for 30–60 min in the presence of $10 \mu\text{g/ml}$ emetine, as described previously (21).

RESULTS

Mitochondria carrying NARP mutant mtDNA were transferred from human fetal fibroblasts to lung carcinoma or osteosarcoma cells that lacked endogenous mtDNA by cell-cytoplasm fusion. The donor mitochondria from fetal fibroblasts contained exclusively mutant (T8993G) mtDNA, and sequencing of the genes encoding ATP synthase subunits 8 and 6 revealed no other novel mutations (data not shown). Mitochondrial transformant cells (cybrids) were selected by their ability to grow in

the absence of uridine, in contrast to ρ^0 cells, which are auxotrophic for uridine (10). Screening of transformant cell lines for the presence of mutant mtDNA revealed that all cybrids examined contained exclusively T8993G mutant mtDNA (data not shown).

Immunoblotting of BN-PAGE and two-dimensional BN-PAGE/SDS-PAGE (Figs. 1 and 2, respectively) with F_1 -ATPase antibody revealed an abnormal amount of sub-complexes of mitochondrial ATP synthase in some lung carcinoma NARP cybrids and all osteosarcoma NARP cybrids examined. These sub-complexes are F_1 -ATPase and a sub-complex, denoted V^* , which contains F_1 -ATPase and an unknown number of copies of subunit c (2, 9). Sub-complex V^* was present in ρ^0 cells (Fig. 1, lane 8, and Fig. 2, lane 4) and must therefore lack subunits A6 and A8, which are encoded in mtDNA. V^* is also known to lack subunit b of F_0F_1 -ATPase (9). Free F_1 -ATPase has been described previously in ρ^0 cells (23) and is known to accumulate together with V^* in cells where mitochondrial translation has been inhibited (2). Interestingly, a sub-complex of ATP synthase has been crystallized recently that comprises F_1 -ATPase and a ring of 10 copies of subunit c (22); however, it is not known if this ATP synthase derivative and V^* are equivalent. All the NARP cybrid cell lines contained at least some fully assembled complex V (Figs. 1 and 2). As the cybrids were homoplasmic for the T8993G NARP mutation, the complex V holoenzyme in these cells must contain mutant subunit 6.

Re-cloning a NARP lung carcinoma cybrid gave rise to sub-clones with an identical pattern of sub-complexes to the parental cell line (Fig. 1), suggesting that the population of cells was homogenous. That is, the result argues against the idea that some cells contained high levels of sub-complexes, whereas others contained exclusively holoenzyme.

Sub-complexes of complex V were present at very low levels or undetectable in three of five NARP lung carcinoma cybrids (clones A, D, and E), two of which are shown in Fig. 2. Where no sub-complexes of complex V were detected, the total amount of complex V holoenzyme was similar in NARP cybrids and control cells, suggesting that there was no significant alteration in the amount of complex V in NARP cybrids. The interclonal variability, in the amount of complex V sub-complexes, among the B2.8993 cybrids may reflect differences in the nuclear gene composition or activity (involving, e.g. assembly factors, chaperones, or nuclear-encoded subunits) among lung carcinoma ρ^0 cells. Such nuclear heterogeneity has been observed previously for osteosarcoma ρ^0 cells (24).

There was some experiment-to-experiment variation in the amount of sub-complexes for a given clone. The extent of the variation is shown in Fig. 3 for osteosarcoma clone 206.8993 A. Note that the relative amounts of all three complexes, complex V holoenzyme, V^* , and F_1 -ATPase, varied not merely the ratio of holoenzyme to sub-complexes. The most common result is shown in Fig. 3, panel 1, where the proportions of holoenzyme, V^* , and free F_1 -ATPase were 75, 12, and 13%, respectively. In the most extreme case, free F_1 -ATPase accounted for approximately half the total H^+ -ATPase (47%), whereas ATP synthase holoenzyme represented only 37% of the total (Fig. 3, panel 3). No such variation was observed in control cells, where holoenzyme always accounted for at least 95% of H^+ -ATPase. These results indicate either that the phenotype fluctuates over time in NARP cybrids or, more likely, that mutant containing complex V is less stable than wild-type ATP synthase. All the NARP cybrid cell lines remained homoplasmic mutant throughout the course of the study. Both the interclonal variability among the lung carcinoma NARP cybrids and the sensitivity to the conditions of isolation and sample preparation of the holoenzyme from the same NARP cybrid point to the crit-

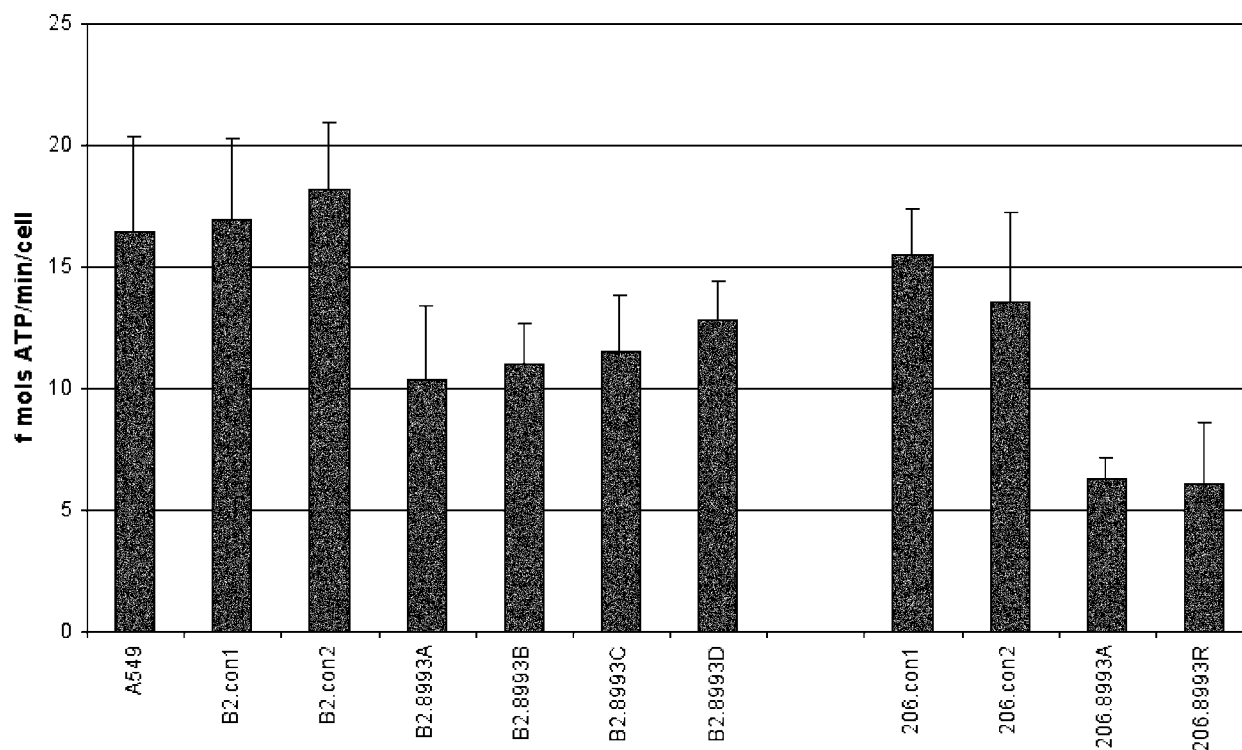


FIG. 6. **ATP synthesis in digitonin-permeabilized NARP cybrids is decreased compared with control cybrids.** ATP synthesis was measured in permeabilized cells in lung carcinoma and osteosarcoma cybrids with 100% NARP mutant mtDNA and cells with no mutant mtDNA, according to the method of Wanders *et al.* (18). The substrate was 5 mM succinate. The values obtained relate specifically to ATP synthesized via respiration, as they were derived by first subtracting the amount of ATP synthesized by the appropriate ρ^0 cell line. A549, lung carcinoma cells; 143B, osteosarcoma cells; B2.8993 and 206.8993 denote, respectively, ρ^0 lung carcinoma cells and ρ^0 osteosarcoma cells repopulated with mtDNA carrying the T8993G transversion associated with NARP. B2.con and 206.con denote ρ^0 cells repopulated with mtDNA of a control subject. Error bars are S.D.

ical role of leucine 156 in the assembly and stability of the ATP synthase complex.

As a further test of the possible effects of the T8993G mutation, [35 S]methionine pulse-chase experiments were performed followed by two-dimensional BN-PAGE of labeled proteins. ATP synthase, F_1 -ATPase, and V^* were distinguishable (Fig. 4), and their relative representation could be deduced by comparing the labeling of α and β subunits of F_1 -ATPase, since these subunits are constituents of all three complexes. First, lung carcinoma NARP cybrids A and D were analyzed, as these did not give appreciable amounts of steady-state sub-complexes. After a 1-h chase, labeled sub-complexes were detected in lung carcinoma NARP cybrid cells, whereas these were largely absent from control cells. In particular, V^* was detectable in lung carcinoma NARP cybrids, whereas labeled V^* was not seen in control cells (Fig. 4A, panels 1–3). V^* was not detectable by immunoblotting in any of the mitochondrial preparations from these lung carcinoma NARP cybrids or controls (Fig. 4B), a finding that established the labeled V^* and F_1 -ATPase as assembly, rather than breakdown, intermediates. We conclude that the transition from V^* sub-complex to ATP synthase holoenzyme is impeded in cells carrying mutant A6. In cells that had been incubated for 3–18 h after removal of [35 S]methionine, almost all the labeled α and β subunits were incorporated into fully assembled complex V in both controls and lung carcinoma NARP cybrids (Fig. 4A, panels 4–6, and data not shown).

A similar assessment of osteosarcoma NARP cybrids also revealed differences between immunoblotting and metabolic labeling analyses. After chases of up to 3 h, the ratio of sub-complexes to holoenzyme was higher for newly synthesized [35 S]methionine-labeled complexes (66:34) than for the steady-state level (30:70) determined by blotting with F_1 -ATPase an-

tibody (Fig. 5, A and B). Thus, although all the newly synthesized (radiolabeled) α and β subunits had been incorporated into ATP synthase holoenzyme in control cells after 3 h, one-third remained as sub-complexes in osteosarcoma cybrids carrying NARP mutant mtDNA. After an 18-h chase, the ratio was similar by both methods in osteosarcoma NARP cybrid and the control cells (Fig. 5, A and B). These findings indicate that the assembly defect was common to both nuclear backgrounds, yet was more marked in the osteosarcoma than the lung carcinoma background given that labeled sub-complexes, which could not be ascribed to disassembly, were detected after a 3-h chase only in the former cell type.

Measurement of ATP synthesis in digitonin-permeabilized cells indicated a decrease of approximately one-third in lung carcinoma NARP cybrids compared with the parental control cell line (Fig. 6). As stated above, some of the cybrids analyzed (B2.8993A and -D) contained few if any sub-complexes on BN-PAGE analysis, like the control cells. Therefore, the ATP synthesis capacity of holoenzyme containing mutant A6 must itself be impaired. The ATP synthesis capacity of osteosarcoma NARP cybrids was approximately half that of control cells (Fig. 6), suggesting that the mutation may be more deleterious in the osteosarcoma nuclear background than that of A549 lung carcinoma cells.

The F_1 -ATPase inhibitory protein (IF_1) is believed to regulate ATP synthase (25, 26); therefore, we tested whether there was a discernible difference between the amounts of IF_1 in control, NARP, or ρ^0 cells. No significant difference was observed (Fig. 7). IF_1 was found to be associated with sub-complexes of ATP synthase as well as with the holoenzyme (Fig. 7). Nevertheless F_1 -ATPase consistently displayed higher in-gel ATP hydrolysis activity than holoenzyme (Fig. 8), suggesting

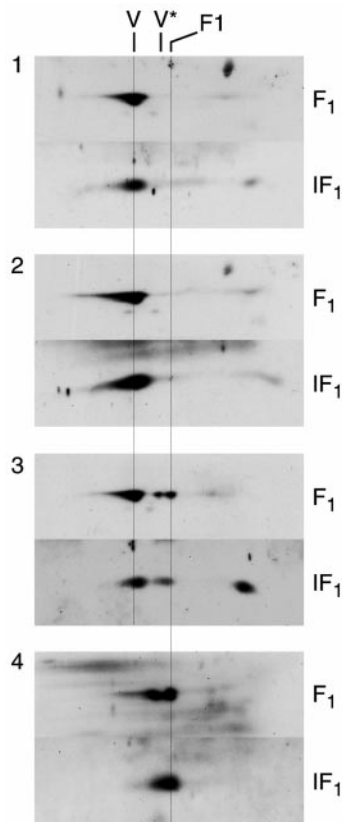


FIG. 7. IF₁ is present in mutant A6 containing ATP synthase holoenzyme in similar amount to controls. Mitochondrial membranes were solubilized and separated by BN-PAGE; after transfer to filters, samples were incubated sequentially with antibodies to the ATP synthase inhibitor protein IF₁ (lower part of each panel) and, after stripping, with antibodies to F₁-ATPase (upper part of each panel). Panel 1, control ρ^+ cells; panel 2, NARP cybrid with no sub-complexes of ATP synthase; panel 3, NARP cybrid with ATP synthase sub-complexes; panel 4, ρ^0 cells. Exposure times were identical for each antibody in panels 1 and 2; therefore, it is concluded that the ratio of IF₁ to F₁-ATPase was similar in NARP cybrids and controls. Two other points of note were the association of IF₁ with free F₁-ATPase of ρ^0 cells (panel 4) and the presence of IF₁ in a novel complex, seen most clearly in panel 3. IF₁ is capable of forming a tetramer (37), yet this complex is considerably larger than 100 kDa and therefore likely involves at least one other protein, perhaps the 21-kDa protein partly characterized previously (38).

that subunits of the F₀ portion of ATP synthase restrict ATP hydrolysis.

Although assays of holoenzyme integrity and the permeabilized cell assay clearly indicated defects of complex V, the T8993G mtDNA mutation had no appreciable phenotypic effect upon intact lung carcinoma or osteosarcoma cybrids. Specifically, there was no significant decrease in oxygen consumption of coupled intact cells carrying T8993G mtDNA compared with controls (Fig. 9). Nor was there any significant increase in lactate-to-pyruvate ratio in spent medium (data not shown). The growth rate of NARP and control cybrids over periods of 7–9 days were indistinguishable, even in medium where galactose was substituted for glucose (data not shown). In contrast, ρ^0 cells and cells with high levels of “A3243G” mutant mtDNA died in galactose medium.³ There was no measurable effect on mitochondrial translation in osteosarcoma cell cybrids with or without T8993G mtDNA (data not shown). In other experiments, incubation with reagents that induce oxidative stress (hydrogen peroxide and menadione) failed to differentiate NARP mutant and control cybrids. Finally, the cellular ATP:

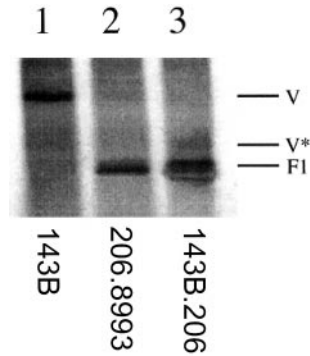


FIG. 8. In-gel assay of ATP hydrolysis revealed higher activity for free F₁-ATPase than ATP synthase holoenzyme. Equivalent amounts of mitochondrial membrane protein were separated as in Fig. 1. After BN-PAGE, ATP hydrolysis activity was measured in-gel according to the protocol of (19). Lane 1, parental osteosarcoma cells; lane 2, an osteosarcoma NARP cybrid; lane 3, osteosarcoma ρ^0 cells. The signal from F₁-ATPase (lane 3) was severalfold higher than that from holoenzyme (lane 1). The absence of signal from the NARP cybrid holoenzyme implies a complete loss of ATP hydrolysis activity; however, this is misleading, as there was a sharp threshold effect for the in-gel assay, *i.e.* loading half the amount of control protein led to complete loss of signal.

ADP ratio decreased dramatically in ρ^0 lung carcinoma cells incubated for 30 min in the absence of glucose, whereas NARP cybrids maintained a ratio similar to control cybrids for at least 4 h (data not shown). Thus, the decrease in ATP synthesis capacity (Fig. 6) and increase in complex V sub-complexes (Fig. 2) in disrupted NARP cells are either of no consequence to growth, even under regimes that favor expression of a functional OP system, or else these *in vitro* observed abnormalities are compensated in intact cells.

The absence of a marked OP phenotype in intact NARP cybrids was mirrored in cybrids containing partially duplicated mtDNA (27). In contrast, earlier studies of A8344G (21) and A3243G mutant mtDNA (28–30) and partial mtDNA deletions (31) demonstrate clear deleterious effects upon OP and mitochondrial translation of intact cybrid cells. Therefore, putative pathological mtDNA mutations cannot be excluded as a cause of disease based on absence of an OP phenotype in cultured cells.

DISCUSSION

Human cells lacking mtDNA have been used widely to study the effects of putative pathological mtDNA mutations (*e.g.* Refs. 8, 21, 24, and 27–32). The genetic outcome of fusing cytoplasm and ρ^0 cells is to transfer mtDNA to a new nuclear background. Thus, mtDNA can be isolated from its host nuclear DNA, and any mitochondrial dysfunction in the transformant cells can be ascribed to mtDNA, where appropriate controls are in place. In this report, mtDNA carrying a presumed pathological mutation in subunit 6 of ATP synthase was transferred to two control nuclear backgrounds to assess its effects on mitochondrial structure and function. In both nuclear backgrounds tested, T8993G mutant mtDNA was associated with decreased complex V assembly and decreased ATP synthesis capacity. Because the effects were observed with NARP mutant mtDNA in two nuclear backgrounds, they can with confidence be attributed to the mutation. Despite these abnormalities there was no marked phenotype in intact cells with mutant ATP synthase. These findings are consistent with what is known of the T8993G mtDNA mutation and its associated diseases. The mutation resides in a gene encoding an essential subunit of ATP synthase and could therefore be expected to affect the intrinsic activity or amount of holoenzyme. Nevertheless, the effects of the mutation must necessarily be subtle,

³ N. Hance and I. J. Holt, unpublished data.

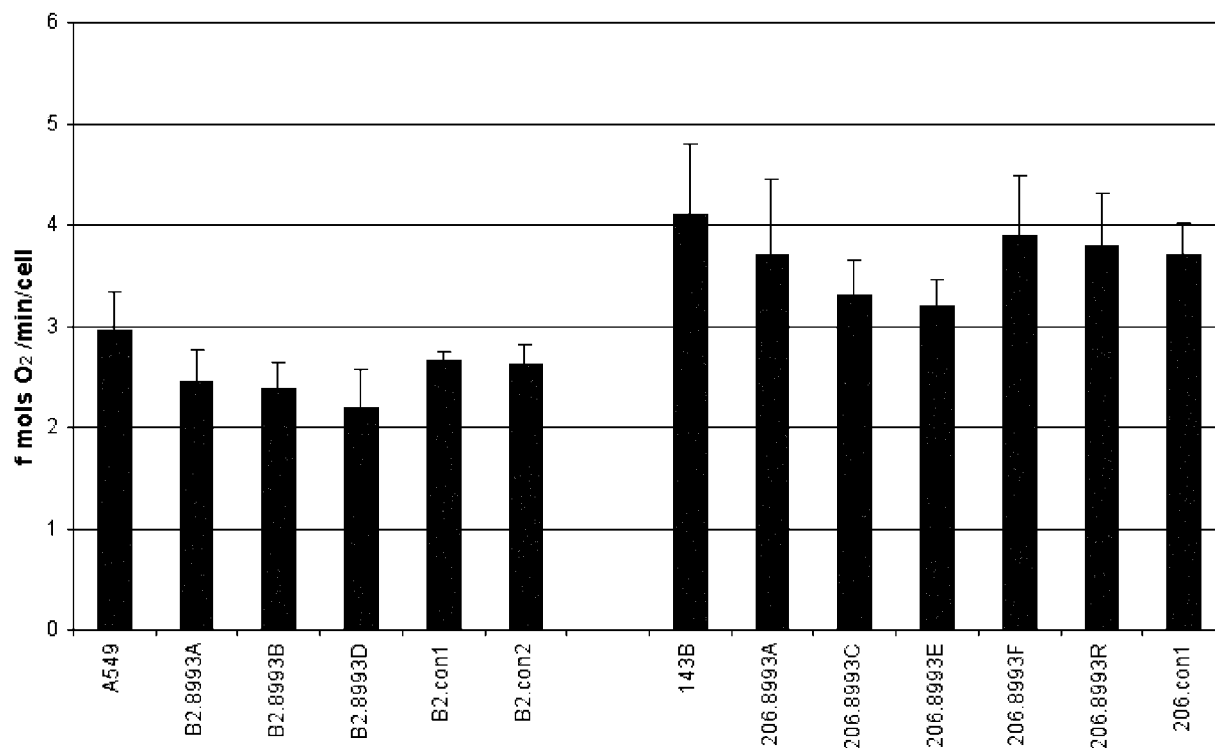


FIG. 9. Oxygen consumption of intact cells carrying T8993G mtDNA was indistinguishable from control cells. Respiratory capacity was measured with a Clark-type oxygen electrode. Cells were harvested and resuspended at a concentration of 5×10^6 cells/ml. A549, lung carcinoma cells; 143B, osteosarcoma cells; B2.8993 and 206.8993 denote, respectively, ρ^0 lung carcinoma cells and ρ^0 osteosarcoma cells repopulated with mtDNA carrying the T8993G transversion associated with NARP. B2.con and 206.con denote ρ^0 cells repopulated with mtDNA of a control subject. Error bars are S.D.

first, because substantial impairment of ATP synthase would be incompatible with life and, second, because the NARP mutation is highly tissue-specific in its effects. For instance, muscle pathology is absent in NARP, whereas it is present in association with a number of other pathological mtDNA mutations.

Early studies assumed that the NARP/MILS (maternally inherited Leigh syndrome) T8993G mutation decreased ATP synthesis capacity directly by impairing proton flux through the F_0 portion of the enzyme, *i.e.* caused a decrease in intrinsic enzyme activity. The finding that the mutation was associated with increased levels of sub-complexes of complex V suggested an alternative explanation, namely that perturbed assembly or stability could lead to a decrease in the total amount of holoenzyme (9). The results reported here indicate that sub-complexes of complex V are often present in isolated mitochondria carrying the mutant form of A6 associated with NARP, yet irrespective of this, ATP synthesis capacity was decreased. Thus, it can be concluded that the function of ATP synthase holoenzyme containing mutant A6 is impaired.

The metabolic labeling experiments indicated that NARP-containing cybrids were impaired in complex V assembly (Figs. 4 and 5). Nevertheless, it is unlikely that all the antibody-detected sub-complexes (Figs. 1–3) represent assembly intermediates; some almost certainly arose via disassembly, given the considerable variation in the ratio of sub-complexes to holoenzyme that was observed (Fig. 3). Therefore, we posit that ATP synthase-containing mutant A6 is not only assembled less efficiently than wild type but also that it is less stable. Instability of mutant-containing holoenzyme might explain much of the reported variation (30–95%) in the degree of impairment of ATP synthesis capacity (Refs. 8 and 33 and this report) and some of the phenotypic difference between intact and disrupted cells. Finally, formation of sub-complexes from disrupted ho-

loenzyme is a reasonable explanation for the observation that there was little complex V holoenzyme in muscle mitochondrial preparations of NARP patients that displayed no muscle pathology (9), *i.e.* it was likely the result of the disassembly. In summary, to reconcile the apparently disparate findings in studies of the T8993G NARP mutation, we propose that complex V-containing mutant A6 has $\geq 70\%$ normal ATP synthesis capacity in intact cells, yet the enzyme is assembled less efficiently and is less stable than that of wild-type cells. Ultimately, it will be necessary to develop a sensitive assay of ATP synthase for intact cells to determine the true extent of enzyme dysfunction in NARP.

Recently it was reported that IF_1 was not associated with F_1 -ATPase of a fibroblast ρ^0 cell line (34), a result that is apparently at odds with the finding reported here. The discrepancy could reflect differences between ρ^0 cell lines, although a more plausible explanation is that the osmotic shock procedure used by Garcia *et al.* (34) had a different effect on the mitochondria of ρ^+ and ρ^0 cells. Indeed, the apparent absence of IF_1 may simply reflect the low yield of F_1 -ATPase obtained by this procedure, as the α and β subunits of F_1 -ATPase were in low abundance in the ρ^0 cell H^+ -ATPase preparation of Garcia *et al.* (34).

The combined ATP synthase abnormalities associated with NARP cybrids might become critical, for example, in particular neuronal cell types or genetic backgrounds, if the cellular environment accentuated the assembly or stability defects or increased ATP synthase turnover. In this context, it is noteworthy that there are differences in brain and muscle in the expression of isoforms of subunit c with which A6 interacts (35). Furthermore, IF_1 is expressed at relatively high levels in developing rat brain compared with muscle (36). This observation suggests that ATP hydrolysis needs to be strictly controlled in developing brain and thereby offers an explanation of

how increased levels of sub-complexes of complex V resulting from the presence of the T8993G mtDNA mutation might cause tissue-specific metabolic failure.

Acknowledgments—I. Holt and L. Nijtmans acknowledge debt to the late Dr. Coby Van den Bogert and the late Professor Anita Harding. We thank Professor H. T. Jacobs for comments on the manuscript and Dr. John Walker who kindly provided IF₁ antibody.

REFERENCES

- Abrahams, J. P., Leslie, A. G., Lutter, R., and Walker, J. E. (1994) *Nature* **370**, 621–628
- Nijtmans, L. G., Klement, P., Houstek, J., and van den Bogert, C. (1995) *Biochim. Biophys. Acta* **1272**, 190–198
- Holt, I. J., Harding, A. E., Petty, R. K., and Morgan-Hughes, J. A. (1990) *Am. J. Hum. Genet.* **46**, 428–433
- Tatuch, Y., Christodoulou, J., Feigenbaum, A., Clarke, J. T., Wherret, J., Smith, C., Rudd, N., Petrova-Benedict, R., and Robinson, B. H. (1992) *Am. J. Hum. Genet.* **50**, 852–858
- Elston, T., Wang, H., and Oster, G. (1998) *Nature* **391**, 510–513
- de Vries, D. D., van Engelen, B. G., Gabreels, F. J., Ruitenbeek, W., and van Oost, B. A. (1993) *Ann. Neurol.* **34**, 410–412
- Tatuch, Y., and Robinson, B. H. (1993) *Biochem. Biophys. Res. Commun.* **192**, 124–128
- Trounce, I., Neill, S., and Wallace, D. C. (1994) *Proc. Natl. Acad. Sci. U. S. A.* **91**, 8334–8338
- Houstek, J., Klement, P., Hermanska, J., Houstkova, H., Hansikova, H., Van den Bogert, C., and Zeman, J. (1995) *Biochim. Biophys. Acta* **1271**, 349–357
- King, M. P., and Attardi, G. (1989) *Science* **246**, 500–503
- Bodnar, A. G., Cooper, J. M., Holt, I. J., Leonard, J. V., and Schapira, A. H. (1993) *Am. J. Hum. Genet.* **53**, 663–669
- Klement, P., Nijtmans, L. G., Van den Bogert, C., and Houstek, J. (1995) *Anal. Biochem.* **231**, 218–224
- Schagger, H., and von Jagow, G. (1991) *Anal. Biochem.* **199**, 223–231
- Schagger, H., Cramer, W. A., and von Jagow, G. (1994) *Anal. Biochem.* **217**, 220–230
- Bradford, M. M. (1976) *Anal. Biochem.* **72**, 248–254
- Nijtmans, L. G., Barth, P. G., Lincke, C. R., Van Galen, M. J., Zwart, R., Klement, P., Bolhuis, P. A., Ruitenbeek, W., Wanders, R. J., and Van den Bogert, C. (1995) *Biochim. Biophys. Acta* **1270**, 193–201
- Nijtmans, L. G., Taanman, J. W., Muijsers, A. O., Speijer, D., and Van den Bogert, C. (1998) *Eur. J. Biochem.* **254**, 389–394
- Wanders, R. J., Ruiters, J. P., and Wijburg, F. A. (1993) *Biochim. Biophys. Acta* **1181**, 219–222
- Zerbetto, E., Vergani, L., and Dabbeni-Sala, F. (1997) *Electrophoresis* **18**, 2059–2064
- Mosmann, T. (1983) *J. Immunol. Methods* **65**, 55–63
- Chomyn, A., Meola, G., Bresolin, N., Lai, S. T., Scarlato, G., and Attardi, G. (1991) *Mol. Cell. Biol.* **11**, 2236–2244
- Stock, D., Leslie, A. G., and Walker, J. E. (1999) *Science* **286**, 1700–1705
- Buchet, K., and Godinot, C. (1998) *J. Biol. Chem.* **273**, 22983–22989
- Chomyn, A., Lai, S. T., Shakeley, R., Bresolin, N., Scarlato, G., and Attardi, G. (1994) *Am. J. Hum. Genet.* **54**, 966–974
- Klein, G., Satre, M., Dianoux, A. C., and Vignais, P. V. (1980) *Biochemistry* **19**, 2919–2925
- Penin, F., Di Pietro, A., Godinot, C., and Gautheron, D. C. (1988) *Biochemistry* **27**, 8969–8974
- Holt, I. J., Dunbar, D. R., and Jacobs, H. T. (1997) *Hum. Mol. Genet.* **6**, 1251–1260
- King, M. P., Koga, Y., Davidson, M., and Schon, E. A. (1992) *Mol. Cell. Biol.* **12**, 480–490
- Chomyn, A., Martinuzzi, A., Yoneda, M., Daga, A., Hurko, O., Johns, D., Lai, S. T., Nonaka, I., Angelini, C., and Attardi, G. (1992) *Proc. Natl. Acad. Sci. U. S. A.* **89**, 4221–4225
- Dunbar, D. R., Moonie, P. A., Zeviani, M., and Holt, I. J. (1996) *Hum. Mol. Genet.* **5**, 123–129
- Hayashi, J., Ohta, S., Kikuchi, A., Takemitsu, M., Goto, Y., and Nonaka, I. (1991) *Proc. Natl. Acad. Sci. U. S. A.* **88**, 10614–10618
- Dunbar, D. R., Moonie, P. A., Jacobs, H. T., and Holt, I. J. (1995) *Proc. Natl. Acad. Sci. U. S. A.* **92**, 6562–6566
- Baracca, A., Barogi, S., Carelli, V., Lenaz, G., and Solaini, G. (2000) *J. Biol. Chem.* **275**, 4177–4182
- Garcia, J. J., Ogilvie, I., Robinson, B. H., and Capaldi, R. A. (2000) *J. Biol. Chem.* **275**, 11075–11081
- Gay, N. J., and Walker, J. E. (1985) *EMBO J.* **4**, 3519–3524
- Sangawa, H., Himeda, T., Shibata, H., and Higuti, T. (1997) *J. Biol. Chem.* **272**, 6034–6037
- Cabezón, E., Butler, P. J., Runswick, M. J., and Walker, J. E. (2000) *J. Biol. Chem.* **275**, 25460–25464
- Lopez-Mediavilla, C., Vigny, H., and Godinot, C. (1993) *Eur. J. Biochem.* **215**, 487–496
- Sambrook, J., Fritsch, E. F., and Maniatis, T. (1990) *Molecular Cloning: A Laboratory Manual*, 2nd Ed., Cold Spring Harbor Laboratory, Cold Spring Harbor, NY